Bandwidth Abundant Optical Networking Enabled by Spatially-Jointed and Multi-Band Flexible Waveband Routing

Hiroshi HASEGAWA[†a)], *Senior Member*

SUMMARY   The novel optical path routing architecture named flexible waveband routing networks is reviewed in this paper. The nodes adopt a two-stage path routing scheme where wavelength selective switches (WSSs) bundle optical paths and form a small number of path groups and then optical switches without wavelength selectivity route these groups to desired outputs. Substantial hardware scale reduction can be achieved as the scheme enables us to use small scale WSSs, and even more, share a WSS by multiple input cores/fibers through the use of spatially-joint-switching. Furthermore, path groups distributed over multiple bands can be switched by these optical switches and thus the adaptation to multi-band transmission is straightforward. Network-wide numerical simulations and transmission experiments that assume multi-band transmission demonstrate the validity of flexible waveband routing.

key words: *flexible waveband routing, node architecture, large scale optical cross-connect, spatial division multiplexing, multi-band transmission*

1. Introduction

The broad bandwidth and rapid technology development of optical networks make these the indispensable infrastructure of our ICT-based society. The ceaseless Internet traffic increase continues with the penetration of cloud-based services including high-resolution video streaming and 5G/6G mobile communications which will enable the digital enterprise, Industry 4.0, and smart cities [1]. Furthermore, the recent COVID-19 pandemic is propelling new programmable broadband data delivery [2]. Thus continuous research and development activities is mandatory to enable future extremely high bandwidth transmission and efficient optical networking.

    The capacity of single mode fibers (SMFs) was enhanced by the successful introduction of dense wavelength division multiplexing (DWDM). After that the digital coherent transmission and the ITU-T flexible grid [3] enabled the pursuit of the maximum frequency utilization efficiency. However, such capacity improvement is now saturating as the achieved capacity is reaching to the theoretical limit [4], [5]. Breaking fresh ground in optical communication would be the use of multiple frequency bands [6]–[11], such as S/C/L (1460–1530 nm/1530–1565 nm/1565–1625 nm), and the introduction of higher spatial parallelism by multi-core fiber /multi SMF links [12]–[17]. The introduction of higher

spatial parallelism has been studied in the context of spatial division multiplexing (SDM) networking where multi core/mode fibers [18], [19], switching devices [20], [21], amplifiers [22], spatial super channels, and node architectures [23] have been developed. Multi-band transmission is attracting attention as the capacity of current SMFs can be substantially increased at the cost of higher transmission loss and the use of switching/amplifying devices covering the wider frequency range.

    Considering the wide deployment and success of conventional hierarchical electrical path networks such as PDH and SDH/SONET, it would be natural to introduce the path hierarchy to optical networks where higher order waveband paths carrying multiple optical wavelength paths are defined. Each wavelength path has to be accommodated by a sequence of waveband paths that bridge the source and destination nodes of the wavelength path. For optical networks that adopt the ITU-T fixed grid, the introduction of path hierarchy has been proposed [24]–[28]; the frequency range available is split equally into several wavebands, and route paths in each waveband are transferred together as a routing entity. The bandwidth uniformity and the regularity of wavelengths in a waveband contribute to reducing the hardware scale of waveband cross-connects; the number of optical switches dedicated to wavebands is reduced and multiplexers/demultiplexers are simplified [29]–[31]. Several studies on designing hierarchical optical path networks that adopt wavebands have been published [24], [26]. Different from conventional hierarchical electrical path networks, a wavelength path has to be accommodated by waveband paths whose waveband covers the wavelength, and a wavelength path cannot go through waveband paths with different waveband indexes even if they are concatenated. These requirements often prevent us from improving the utilization ratio of waveband paths and degrade the hardware scale reduction achievable by adopting the path hierarchy. Moreover, the above definition of path hierarchy is not valid for the latest ITU-T flexible grid optical networks with wavelength selective switch (WSS) based optical cross connect (OXC) nodes as the path bundling does not have any impact on the number of ports at WSSs and there is no regular structure if the bundled paths have disparate bandwidths.

    Several recent proposals introduce and combine fiber granularity routing with path granularity add/drop and/or grooming. The resulting configuration corresponds to a variant of coarse granularity routing optical networking where the bandwidth of waveband equals the bandwidth available

in a fiber and the number of wavebands is set to one. These networks are valid for the ITU-T flexible grid and escape the difficulty posed by traversing sequences of waveband paths due to the waveband index difference. Fiber granularity routing allows us to employ optical switches that are wavelength insensitive. Such switches can be very scalable [32] and provide better transmission characteristics in terms of loss and filtering impairment as well. The filtering impairment mitigation enables us to adopt higher WDM densities [33]. However, the resulting inflexibility such that all paths in a fiber must pass to the same next fiber severely degrades the fiber utilization efficiency.

For the hardware scale reduction of flexible-grid-ready OXC nodes while keeping sufficient routing flexibility, we have proposed the architecture named flexible waveband routing networks [34]–[38]. The proposed flexible waveband routing node adopts a two-stage switching scheme where WSSs at the input sides bundle optical paths, and then optical switches route these path groups to the output ports. Paths in each bundle can be any combinations of paths in the input fiber, regardless of their center frequencies and bandwidths, thus we refer to these bundles as flexible wavebands. Here flexible wavebands are routing entities defined on each fiber, and no higher order waveband path is defined in a network. The number of wavebands per fiber can be small (2~4) to achieve similar routing performance to conventional networks. This paper shows that coarse granularity routing networks, hierarchical optical path networks, fiber granularity routing networks, and flexible waveband routing networks, can define sparse meshes or line/ring/tree shaped sub-networks, on which each optical path is routed. We explain how the tree-shaped sub-networks defined by flexible waveband routing provide much greater routing flexibility. We also introduce a network design algorithm based on graph-degeneration; it simultaneously optimizes path routing and switching state of optical switches for flexible waveband routing. We verify that the routing performance of the proposed flexible waveband routing node basically matches that of conventional WSS-based OXC nodes on typical core/metro network topologies. A routing performance verification and C+L multi-band transmission experiments on a prototype are shown in the last part of this paper to elucidate the validity of flexible waveband routing networks.

This paper is organized as follows. The scalability issue of conventional WSS-based OXCs is summarized and then the introduction of coarser granularity routing aiming at hardware scale reduction is reviewed in Sect. 2. Then the proposed optical path routing scheme and the flexible waveband routing node architecture are explained in Sect. 3. Validity of the proposal is verified through numerical evaluations and transmission experiments. Finally, the conclusion is shown in Sect. 4.

2. Preliminaries

In this paper, we assume that optical paths are set on the

ITU-T flexible grid and multiple frequency bands can be used. Each link between an adjacent node pair consists of multiple single-mode fibers or multi-core fibers (MCFs). For notational simplicity, we assume that each optical path is accommodated by one of the fibers/cores on each link. However, spatial super-channels can be accommodated in flexible waveband routing networks.

Large-scale WSS-based OXC nodes whose degrees exceed these of the WSSs used necessitate the cascading of WSSs; however, WSS number is basically the square of node degree. If we adopt WSSs for different frequency bands for multi-band transmission, the minimum degree among these WSSs characterizes node scalability. These scalability issues will be explained in detail in Sect. 2.1. Thus we have to develop a node architecture that can limit the degree of WSSs to a small integer. In Sect. 2.2, we provide a survey on optical path networks which aim at OXC scale reduction by introducing bundled path routing. Then we explain how routing performance deterioration does occur with the path bundling schemes proposed in conventional studies.

2.1 Scalability Issue of Optical Cross-Connects

Existing optical cross-connects consist of WSSs that can distribute (/combine) WDM signals from the input (/output) to the output (/input) as shown in Fig. 1. The output port of a signal can be arbitrarily selected independent from the routing status of the other signals. A WSS is not only able to route each signal but also implement add, drop, and VOA functionalities for all signals. Thus WSSs play key roles in current OXC nodes.

Although WSSs are universal devices for routing in the optical domain, we have to consider their attributes including loss, valid frequency range, and available degree. If we assume that the loss while traversing a WSS is 7 dB, the total loss to traverse two WSSs located at input and output will be 14 dB which is acceptable given the wide availability of EDFAs with 20+dB gain. If the degree of an OXC is less than or around 10x10, either WSSs at the input or these at the output can be replaced by optical splitter/couplers and the total cost of the optical cross-connect can be almost halved.

The available degrees of WSSs are 1x4, 1x9, 1x20 and recently 1x30+, but cost increases with the degree. Small-scale OXCs such as 9x9 can be realized cost-effectively as
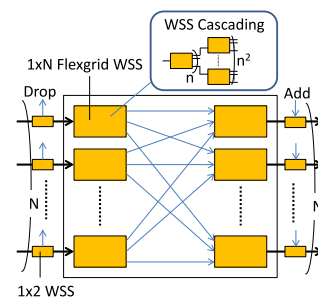

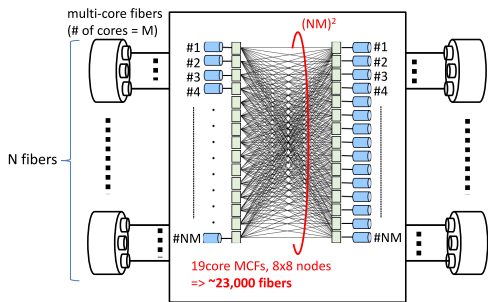**Fig. 1** WSS-based optical cross-connect (route-&-select configuration).
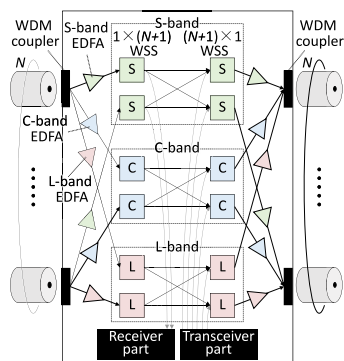
Fig. 2   Fully flexible OXC for SDM networks.

Fig. 3   OXC for Multi-band networks.

(a) Insertion of additional EDFAs

(b) Normalized numbers of WSSs and EDFAs

Fig. 4   Hardware scale explosion at WSS-based OXCs.
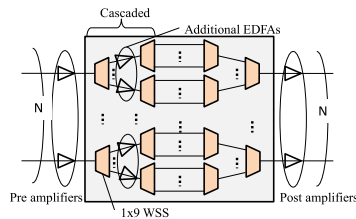
the use of low degree WSSs and optical couplers/splitters is allowed. However, the steep traffic growth necessitates incremental growth in OXC degree. Higher WSS degree is essential for higher degree optical cross-connects. Recent studies on the introduction of spatial parallelism and the use of multiple frequency bands could necessitate larger scale OXCs.
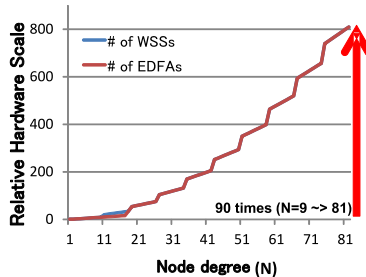
Different types of multi-core fibers have been studied with cores of 4, 7, 19, and so on. OXC node architectures to bridge such multi-core fibers were summarized in [23]. The most flexible node configuration uses large-scale OXCs that can accept all cores in parallel (Fig. 2). However, as the number of cores connected to the input (/output) side is the product of number of input (/output) fibers and the number of cores in each MCF, node scale will be unacceptably large.

The valid frequency range of a WSS is limited to the most constrained of the frequency bands, S/C/L, or multiple bands such as C+L. Consider the case that each WSS could cover only one of the bands to be used. Then multiple OXCs dedicated to each band should be installed and sandwiched by WDM couplers (Fig. 3). OXC degree would be bounded by the highest WSS degree available for these bands.

The concatenation of WSSs can increase WSS degree (Fig. 1); unfortunately, this not only increases the number of WSSs necessary, but also worsens the loss. The number of WSSs in a large-scale OXC is almost the square of its degree. A signal traversing a node with concatenated WSSs may need to go through 4 WSSs; if each WSS traversal causes 7 dB loss, the total loss reaches 28 dB, necessitating the use of additional amplifiers. Figure 4 shows the number

of pre-/post-/additional amplifiers needed for optical cross-connects [35]. It elucidates that the number of amplifiers is also the square of the degree of the OXC.

The above discussions show the need for developing scalable OXCs that can accommodate many optical fibers/cores while achieving acceptable hardware scale.

2.2   Routing Granularity and Path Hierarchy

The introduction of path optical hierarchy to simplify OXCs was discussed in the 2000s' drawing on the analogy of SDH/SONET networks. In the 2000's, OXCs were assumed to consists of multiplexers, demultiplexers and matrix switches dedicated to wavelengths (Fig. 5). Optical paths located on the regular grid standardized by ITU-T are regularly grouped and these groups are referred as wavebands. OXCs for path/waveband hierarchical routing form stacked OXCs as shown in Fig. 6. The lower OXCs are responsible for waveband granularity routing while the upper ones handle path granular routing and add/drop/VOA. As waveband granularity routing enables a switch to route a bundle of paths together, the total switch scale can be reduced provided most path routing involves waveband granularity. Each optical path will traverse one or a sequence of concatenated multiple waveband paths. The operation to route optical paths in a waveband path terminated at the node to the other waveband paths starting from the node is called grooming and is mandatory in networks with path hierarchy; without grooming, waveband paths will be sparsely utilized and the utilization efficiency of network capacity will be severely degraded.

In SDH/SONET networks, a lower order path can be accommodated by any sequence of concatenated higher order paths bridging the source and destination nodes of the lower order path. However, waveband paths are associated with dif-
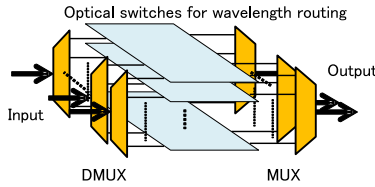
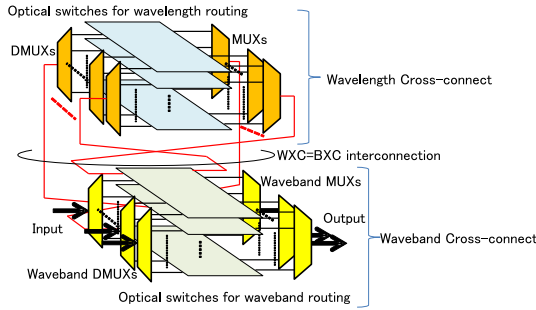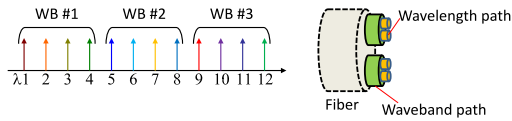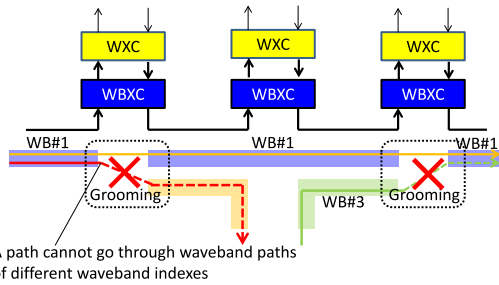**Fig. 5** OXC for fixed grid optical path networks.

Fig. 6 OXC for hierarchical optical path networks.
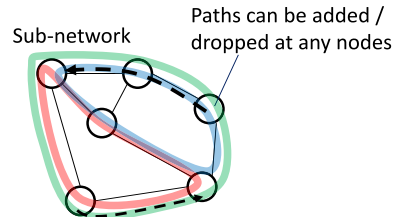

(a) Waveband configuration
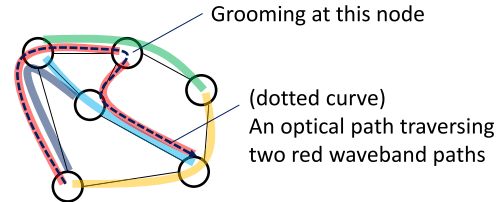

(b) Wavelength path traversing multiple waveband paths

Fig. 7 Waveband continuity constraint in hierarchical optical path networks.

(a) Ring-shaped sub-networks defined by Grouped routing.

(b) Sparse mesh defined by waveband paths.

Fig. 8 Path accommodation to coarse granularity routing optical networks.

Fig. 9 Waveband cross-connect node that consists of waveband selective switches (WBSSs) and WSSs.

ferent frequency ranges (indicated by the waveband indexes) and an optical path can traverse the waveband paths that cover the frequency occupied by the optical path (Fig. 7). Therefore, grooming operations are infrequent in optical networks with path hierarchy. Moreover, additional ports are needed to bridge two different OXCs in a node for add/drop/VOA through hierarchical optical cross-connection. Grooming increases the number of additional ports which enlarges the OXC; thus the use of grooming should be avoided provided waveband paths can be sufficiently filled with optical paths.

Figure 8(a) shows path accommodation in hierarchical optical path networks; waveband paths define sparse meshes in the network and paths go through a mesh covering their source and destination nodes. Grooming is necessary to traverse multiple links in each sparse mesh; each link of a mesh corresponds to multiple physical links in the original
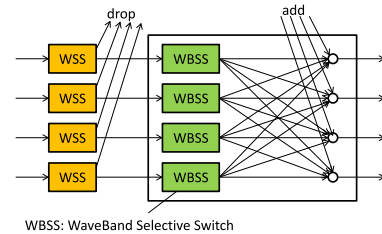
networks and the number of nodes included in a mesh is small. These meshes must be sparse as optical paths have to be routed mostly by waveband cross-connects.

An alternative approach that takes advantage of coarse granularity routing is our grouped routing network architecture; path routing is done at the waveband granularity level while add/drop/VOA operations involve path granularity. The node architecture for grouped routing networks is shown in Fig. 9 where a waveband routing OXC is located in the middle and small degree WSSs and optical couplers are located at the input and output sides. As the hierarchical optical path networks and the grouped routing networks adopt routing in the waveband granularity, we refer a class of networks with bundled path routing coarse granular routing hereafter.

Unlike path accommodation in hierarchical optical path networks, see Fig. 8(b), optical paths in grouped routing networks traverse ring and/or linear subgraphs defined by waveband routing. A path must be carried by one of the subgraphs and can be added/dropped at any node on the subgraph. The design task posed by this class of networks is to find an appropriate set of subgraphs that can cover node pairs to which optical paths will be established. The implementation of grouped routing to conventional networks with WSS-based OXCs has been studied with the goal of higher density in wavelength division multiplexing; please see [42], [43] for

details.

These network types adopt different routing philosophies; however, both necessitate the covering of node pairs by certain subgraphs; sparse mesh sets for hierarchical optical networks and sets of rings and lines for grouped routing networks. The inflexibility created by node pair covering has to be reduced while taking advantage of coarse granular routing. The use of fiber granularity routing instead of waveband granularity routing has been discussed recently [33], [39]–[41]. The fiber granularity routing is a special case where the number of wavebands in a fiber is set to one. The waveband continuity constraint shown in Fig. 7(b) can be ignored. We can introduce large-scale optical switches for fiber granularity switching to improve transmission impairment and switch scale. Indeed, as the scale of large optical switches exceeds 500x500 [32], such large scale nodes can be realized in theory; however, severe routing performance deterioration occurs in dynamic network operation cases [41].

3. Flexible Waveband Routing Networks

3.1 Node Architecture and Routing Scheme

Hierarchical optical path networks and grouped routing networks split the frequency band into several wavebands and group optical paths in each waveband. However, this path grouping approach does not suit the latest ITU-T flexible grid as optical paths may occupy the grid position on waveband boundaries. In order to realize coarse granularity routing that supports arbitrary bandwidth paths and enables hardware scale reduction, we proposed the coarse granularity routing network architecture named flexible waveband routing networks. Unlike conventional networks where WSSs contribute to selecting the output/input fibers of an OXC node for each path, WSSs are used as flexible demultiplexers/multiplexers to form groups of arbitrarily selected paths (Fig. 10). Here the WSSs do not directly contribute to path routing. Optical switches in the middle are responsible for routing of grouped paths. The degree of WSSs used defines the number of path groups, the number of flexible wavebands, which stands for the number of optical matrix switches necessary, and thus routing flexibility.

Let's verify how path grouping and branching at nodes impact the node pair covering discussed in the last part of the previous section. Assuming that the number of flexible wavebands is two, the maximum number of nodes that can be accessed within n hops is $2^{n+1} - 1$ (See Fig. 11(a)). If $n = 10$, then the number of nodes covered reaches 2047. As the numbers of nodes of typical topologies will not exceed 30, all the node pairs can be covered by a tree defined by branching at nodes. This simple example shows how the branching capability makes the flexible waveband routing superior to conventional fiber/core granular routing. If merging is allowed at nodes, then multiple trees can share sub-trees (See Fig. 11(b)). Thus merging operations can improve the routing performance further with further enhancement by replacing matrix switches with distribute-&-coupling (DC)
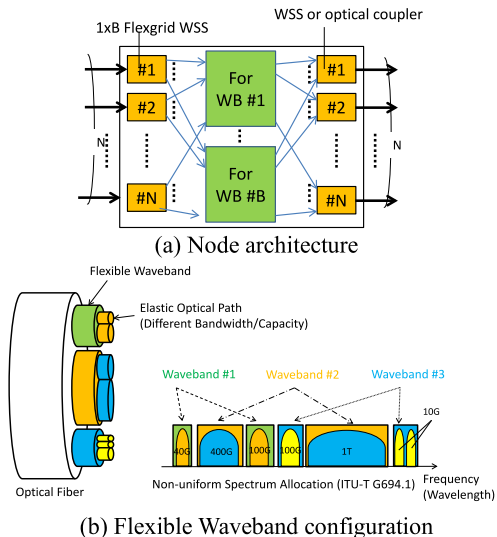

(a) Node architecture

(b) Flexible Waveband configuration

Fig. 10   Flexible waveband routing.

(a) Number of nodes covered by a tree (B=2)

(b) Sub-tree sharing between multiple trees defined by flexible waveband routing.
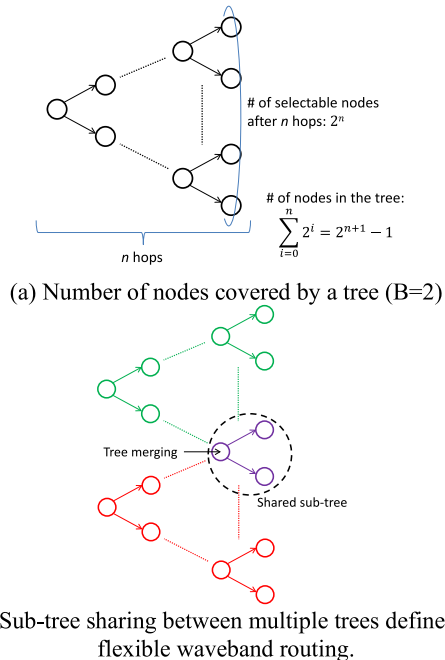
Fig. 11   Trees defined by flexible waveband routing.

type matrix switches, which allows signals from multiple input ports to be merged at the same output port.

3.2 Designing Flexible Waveband Routing Networks

Network design algorithms have to be developed for flexible waveband routing networks as the routing capability of nodes is different from that of WSS-based conventional nodes. The objective of network design is to establish all paths, which are requested in advance, and to minimize some given cost metric. Typical cost metrics are the number of fibers necessary or the total cost incurred to provide the nodes and fibers in the network. Hereafter, we focus on minimizing the to-

tal number of fibers. In conventional WSS-based networks, the minimization of fiber number is formulated as an Integer Linear Programming problem; however, the complexity of the problem is too high to find the optimal solution for networks with 20+ nodes. Indeed, it has been verified that minimization of fiber number is NP-complete [44].

As the minimization of fiber number for flexible waveband routing optical networks is still a complex optimization problem, with the additional constraint that the set of paths in an input fiber has to be bundled into a small number of path groups. The typical approach to designing large scale conventional optical networks is to adopt path-by-path sequential accommodation. That is, for a pair of given topology and a set of path setup requests, pick up requests one by one and accommodate it on the topology with an appropriate pair of route and wavelength/spectrum. Fibers are installed only when they are necessary to accommodate the path; fiber number increment is avoided as much as possible. This simple algorithm can be applied to design large scale networks with 50+ nodes. We have applied a variant of this algorithm to the design of flexible waveband routing networks whose nodes adopt DC-type matrix switches where wavebands can be merged at the output ports [34]. Almost comparable routing performance is assured even if the waveband number is set to a small integer.

The initial design algorithm shown above relies on the flexibility in the number of wavebands merged at output ports. We have tried to apply the algorithm to design flexible waveband routing networks without DC-type matrix switches, but without success. This is because bounding the number of wavebands accepted by an output port often prohibits trees from using that port. Thus we need to develop another algorithm that enables optimization of the number of wavebands at both input and output ports. In [38], we proposed an algorithm based on iterative graph-degeneration. The algorithm is summarized below.

⟨Flexible waveband routing network design based on iterative graph-degeneration⟩

Step 1. For given topology and a set of path setup requests, use path-by-path sequential accommodation to design an initial network consisting of conventional nodes.

Step 2. Construct a large-scale graph where sub-graphs representing nodes are bridged by links that correspond to fibers. Each subgraph is a bipartite graph and stands for the interconnection between input and output ports in the node. A fixed weight value, e.g. 1, is assigned to each link bridging a pair of subgraphs. Small positive values, e.g. 0.01, are assigned to all links of all subgraphs. Determine positive integer i_{max} that bounds the number of iterations.

Step 3. Sort the path setup requests in descending order of hop counts of shortest routes from their source to destination nodes. If there are multiple requests with the same hop count value, then their order is selected randomly. Accommodate all the paths on the network by path-by-path sequential accommodation with minimum weight routing.

Step 4. For each pair of input and output ports of a node,

count the number of paths going through the pair. Increase the weight value of a link in the corresponding subgraph if the number of paths traversing the link is not sufficient. This change encourages paths to concentrate on a small number of subgraph links. If the numbers of wavebands in all nodes satisfy the given bound, terminate. If the number of iterations of Steps 3–4 exceeds bound i_{max}, install additional fibers to reduce the number of wavebands and reenter Step 2. Otherwise remove all the paths from the network and go back to Step 3.

Remark The large-scale graph constructed in Step 2 represents all the fiber interconnections in the network except for add/drop portions. Here we assume so-called full C/D/C add/drop capability, and we do not consider interconnection at that port. However, if we do want to discuss the hardware scale reduction by relaxing the add/drop capability, for example degradation of C/D add/drop functionality, then the interconnection of the add/drop portion can be attached to the large-scale graph and the degeneration imposed by interconnection of the add/drop portion can be tackled together with the optimization of flexible waveband routing at OXCs.

### 3.3 Adaptation to Spatial Division Multiplexing by Spatially-Jointed Path Grouping

The two-stage switching scheme in flexible waveband routing nodes offers efficient adaptation to latest transmission technologies, spatial division multiplexing and multi-band transmission. For the adaptation to the former, we adopt spatial joint switching mode at WSSs while that for the latter we adopt a parallelization of WSSs covering different bands to realize path grouping over multiple bands. As the strategies for the adaptations are different, these to the former and the latter are respectively described in Sect. 3.3 and Sect. 3.4.

Spatial joint switching mode at WSSs has studied so far to reduce the number of WSSs necessary at an SDM node by sharing a WSS among all cores of a MCF. The drawback of the spatial joint switching mode is that WSS degree is quite limited. For example, a 1x20 WSS can be used as a 7-core 1x2 WSS. For conventional WSS-based nodes, cascading WSSs will be mandatory to increase the degree; however, we can adopt small degree WSSs for path grouping in flexible waveband routing networks. Figure 12 shows how optical paths in a multi-core fiber will be grouped for the spatially jointed flexible waveband networks. Same frequency band splitting is applied to all cores and once wavebands are formed in all cores, then wavebands in each core will be routed independent from the routing in the other cores. As the number of cores in a MCF increases, the number of MCFs connected to a node can be kept small if we assume the traffic volume is the same. Thus more switches with smaller degree become possible.

Figure 13 illustrates the routing performance comparison and the hardware scale reduction made possible with the introduction of spatially jointed flexible waveband routing on the 5x5 regular mesh networks [37]. The number of cores
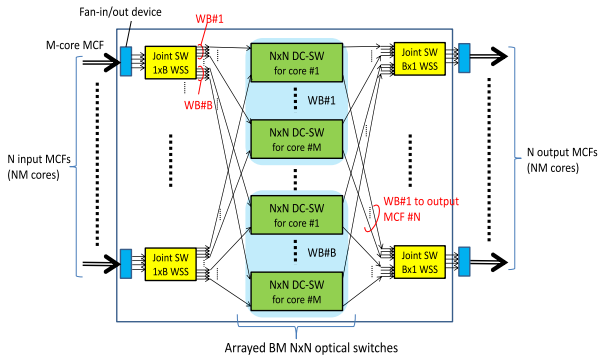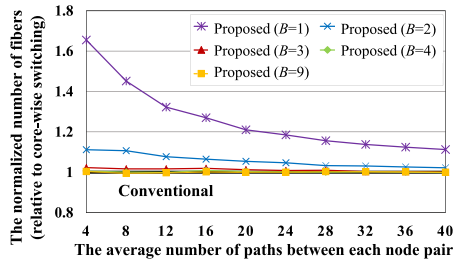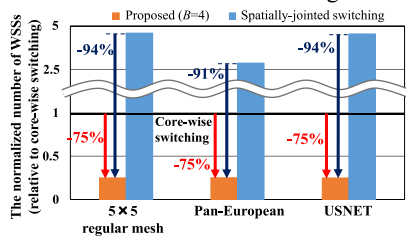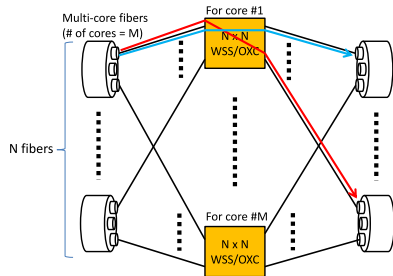
(a) Node architecture
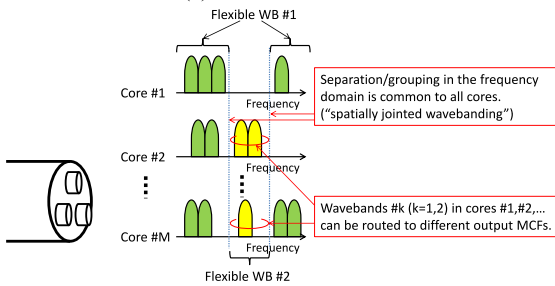
(b) Waveband formulation

Fig. 12   Spatially jointed waveband routing.

(a) Fiber number variation on 5x5 regular mesh.

(b) WSS number reduction relative to core-constrained node and spatially-jointed switching OXC node on different topologies.

(c) Core-constrained node

Fig. 13   Routing performance and hardware scale evaluations for spatially-jointed flexible waveband routing networks.
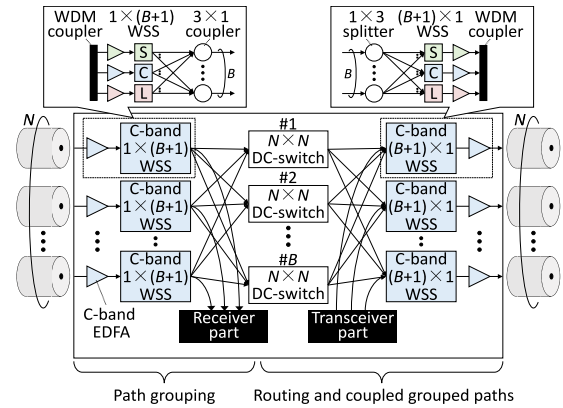

Fig. 14   Multi-band flexible waveband routing node.

in a MCF is set to 4. The baseline is core-constrained OXC nodes, where an OXC is dedicated to each core and paths have to go through same core (See Fig. 13(c). The core-constraint nodes can achieve a substantial hardware scale reduction and an almost equivalent routing performance to the fully flexible WSS-based OXC nodes. We also adopt another alternative called spatially-jointed OXC nodes where WSSs of fully flexible WSS-based nodes are replaced by WSSs of spatially jointed switching modes. As we noted in the previous paragraph, the cascading of WSSs is mandatory and numerous WSSs are used. The relative number of fibers necessary in the network is shown in Fig. 13(a). The increment in the number of wavebands improves the routing performance of flexible waveband routing networks. By setting B=2, the worst gap to the core-constrained node is ~10% and become the negligible when B=4. Figure 13(b) is the hardware scale comparison with the core-constrained and the spatially jointed switching OXC nodes. The hardware scale reduction reaches to 75+% for all cases.

3.4   Adaptation to Multi-Band Transmission

As WSSs are separated from optical switches and optical switches can route paths in flexible wavebands together regardless of their wavelengths, we can adapt the flexible waveband routing node to multi-band transmission by replacing each WSS with an arrays of multiple WSSs covering different frequency bands. In each WSS group, WSSs are arrayed in parallel and their inputs and outputs are bridged by WDM couplers (See the boxes in Fig. 13). The combination of WSSs can be changed according to the availability of WSSs; for example, we can combine WSSs for C+L bands and S-band. We do not need high port count WSSs here, and hence, higher availability of WSSs for different bands is expected. The losses at WDM couplers are added to the total loss for each traversal of a node. Figure 14 shows the multi-band node configuration proposed in [38] where multi-input multi-output couplers/splitters are used to reduce the loss.

Table 1 Network parameters.

Network topology	(a) 4×4 regular-mesh	(b) Kanto	(c) US-metro
# of nodes	16	11	29
# of links	24	18	41
Max. node degree	4	5	7
Ave. node degree	3	3.27	2.83

Fig. 15 Normalized number of necessary fibers relative to WSS-based node.

Fig. 16 Configuration for transmission experiments.

4. Performance Evaluations

In this section, we elucidate the validity of flexible waveband routing networks by network-wide analysis involving numerical simulations and transmission experiments. The results shown here originally appeared in [38]; nodes with standard matrix switches without coupling capability are assumed. We also have demonstrated the performance of nodes with DC-type matrix switches [34]–[37]. For example, as briefly shown in Sect. 3.3, we adopt the spatially joint switching mode at WSSs for spatially jointed flexible waveband routing and WSS number minimization (See [37] for detail).
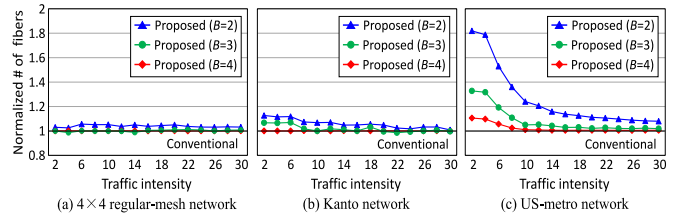
4.1 Numerical Simulations

The following topologies are used; a 4×4 regular-mesh network, Kanto (Tokyo metropolitan) network, and US-metro network with, respectively, 16 nodes/24 links, 11 nodes/18 links, and 29 nodes/41 links (See Table 1). Single mode fibers are laid on links so as to accommodate the optical paths to be setup. We assume C+L band transmission where the total frequency width of each fiber is 9.6 THz divided into 768 12.5 GHz width frequency slots.
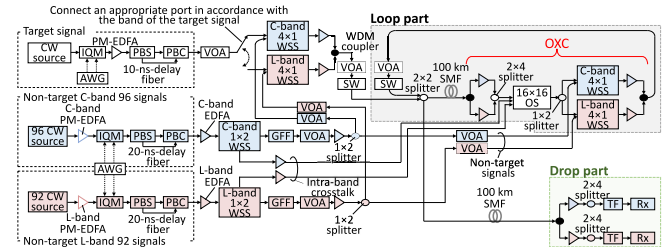
We assume a uniform traffic distribution; source and destination nodes are randomly selected from all nodes following a uniform distribution. The number of optical paths to be setup in the network is controlled by changing the traffic intensity parameter which represents the expected number of paths between each node pair. Three different path capacities are assumed; 100 Gbps, 400 Gbps, and 1 Tbps occupying 4, 7, and 15 slots, respectively. A uniform path-occurrence probability is used; e.g. 33.3% for each capacity.

The benchmarking alternative is the network consisting of conventional nodes with high-port count WSSs. For flexible waveband routing networks, conventional matrix switches are used and the number of wavebands, B, is set to 2–4. Thus waveband merging is not possible at matrix switches. The metric for evaluations is the number of fibers necessary to accommodate the above path setup requests. The results shown in this paper are ensemble averages of 20 simulations.

Figure 15 shows the variation in the number of fibers with traffic intensity change. The fiber number ratio incre-

ment in small traffic volume is shown. This is because the number of accessible adjacent nodes is small if few fibers are set on each link. Thus the increment becomes small if we adopt larger B. However, even if we adopt small B, the increment is gradually reduced as more fibers are set on a link. The fiber number ratio increment in the high-traffic-intensity area is less than 8% for all topologies. If B is set to 3, the increment is less than 2%, and almost negligible if B is set to 4. The fiber number ratio increment for US-metro is more obvious than for the other topologies. This could stem from the structure of US-metro such that the edge areas are not bridged by links and are connected only to the center area. Thus higher routing flexibility is essential in the center area.

4.2 Transmission Experiments

In this subsection, we review the transmission experiment that measured the BERs [38] after 1000+km traversal. Figure 16 shows the experimental configuration.

At the transmitter side, a continuous wave (CW) was generated by a tunable laser. The CW was modulated to 32 Gbaud 4QAM signal by a lithium-niobate IQ modulator (IQM) driven by an arbitrary-waveform generator (AWG). Next, the signal was amplified by a polarization-maintaining (PM) erbium-doped fiber amplifier (EDFA). Then, the DP-4QAM signal was generated by a polarization-division multiplexing (PDM) emulator consisting of a polarization-beam splitter (PBS), a 10-ns-delay fiber, and a polarization-beam combiner (PBC). As non-target signals, 188 wavelength 32 Gbaud DP-4QAM signals were generated by using a 188-CW source, an IQM, and a PDM emulator, where 96-wavelength signals and 92-wavelength signals were aligned on a 50 GHz grid in the C-band and L-band, respectively. The total frequency range reached 9+ THz. After amplification by ED-FAs, a signal on the same wavelength as the target signal was
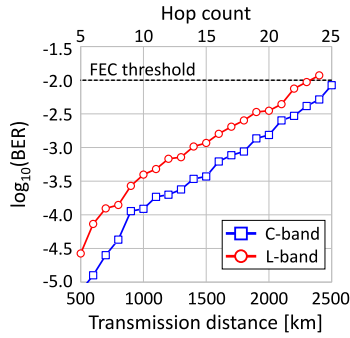
Fig. 17   BER variation subject to the number of hops.

extracted by a 1×2 WSS and used as intra-band crosstalk. The 1x2 WSS represents the add portion of the source node. The power of the non-target signals was flattened by gain-flattening filters (GFFs) and adjusted by variable optical attenuators (VOAs) and EDFAs. The non-target signals were split by 1×2 splitters and were added to optical nodes. The target signal and the non-target signals were merged in 4×1 WSSs and a WDM coupler yielding a 188 channels each with a 32 Gbaud DP-4QAM signal. Signal power was controlled by EDFAs and VOAs. Here a pair of WSSs was adopted to support C and L bands to demonstrate how devices in the node can be parallelized. As any combination of WSSs is possible, the generalization to the case with different combination of bands such as S/C/L is straightforward.

The signals were injected into a loop consisting of a 2×2 optical splitter, a 100km SMF, the OXC under test, a VOA, and two synthesized switches (SWs). The loss coefficient and nonlinearity coefficient of the SCF were 0.18 dB/km and 1.5/W/km, respectively. The dispersion parameter of the SCF in the C-band and L-band was 16.3 ps/nm/km and 18.9 ps/nm/km, respectively. The OXC consisted of a WDM coupler, a C-band EDFA, a L-band EDFA, a 2×4 splitter, a 16×16 optical selector, a 1×2 splitter, a C-band 4×1 WSS, a L-band 4×1 WSS, a C-band EDFA, a L-band EDFA, and a WDM coupler. The noise figures of the C-band and L-band EDFAs were around 5 dB and 6dB, respectively. After looping multiple times, the signal route was switched, and the signals entered a 100 km SMF. Finally, signals were dropped by a 2×4 splitter, an optical tunable filter (TF), and coherently detected.

Figure 17 plots the BER versus hop count in the C-band and L-band transmission. The acceptable BER was set to 10^{-2} as we assume the use of forward error correction (FEC). We observed the C-band and L-band signals could be transmitted 25 hops/2500 km and 23 hops/2300 km, respectively. Thus, we confirmed that the proposed node can be applied to most metro networks including the topologies shown in Table 1. Note that this experiment was conducted under the worst case where the signal is impaired due to spectrum narrowing at every node. If we use fewer hops and multiple fiber spans, the spectrum narrowing effect becomes less and the transmissible distance will be extended.

5.   Conclusions

A novel optical path network architecture named flexible waveband routing networks was reviewed; its design involved a two-stage path routing scheme with WSSs and optical switches. Each WSS bundles incoming paths into a small number of groups to be routed to different output fibers whereas conventional fiber granularity routing cannot distribute paths to different fibers. This distribution mechanism provides sufficient flexibility in routing. Substantial hardware scale reductions and support of spatial division multiplexing and multi-band transmission were achieved. Its validity was demonstrated through numerical simulations and transmission experiments; for example, a 4x4 node prototype with 21-core spatial joint switching capability demonstrated 2.15 Pbps throughput for the fully equipped node and a node prototype with multi-band switching capability was developed; transmission over 2000+ km was verified. In addition to the improvement in terms of node architecture and algorithms to pursuit cost-effectiveness, for the introduction of flexible waveband routing networks, further studies have to be done for example on the resiliency of flexible waveband networks against complex multiple failures, the performance evaluation in dynamic path operation scenarios, and the implementation of modular growth capability of flexible waveband routing nodes to realize cost-effective network capacity expansion.

References

[1] Cisco Systems, Inc., "Visual networking index: Forecast and trends, 2017–2022," White paper, 2019.

[2] Ministry of Internal Affairs and Communications, Telecommunications Division Data Communication section, 2021. https://www.soumu.go.jp/main_content/000791761.pdf

[3] ITU-T Recommendation G.694.1, Spectral grids for WDM applications: DWDM frequency grids, 2021.

[4] R.-J. Essiambre, G. Kramer, P.-J. Winzer, G.-J. Foschini, and B. Goebel, "Capacity limits of optical fiber networks," J. Lightwave Technol., vol..28, no.4, pp.662–701, 2010.

[5] R.-J. Essiambre and R.W. Tkach, "Capacity trends and limits of optical communication networks," Proc. IEEE, vol.100, no.5, pp.1035–1055, May 2012.

[6] A. Mitra, D. Semrau, N. Gahlawat, A. Srivastava, P. Bayvel, and A.

Lord, "Effect of channel launch power on fill margin in C+L band elastic optical networks," IEEE/OSA J. Lightwave Technol., no.38, vol.5, pp.1032–1040, 2020.

[7] N. Sambo, A. Ferrari, A. Napoli, N. Costa, J. Pedro, B. Sommerkorn-Krombholz, P. Castoldi, and V. Curri, "Provisioning in multi-band optical networks," IEEE/OSA J. Lightwave Technol., vol.38, no.9, pp.2598–2605, 2020.

[8] D. Uzunidis, E. Kosmatos, C. Matrakidis, A. Stavdas, and A. Lord, "Strategies for upgrading an operator's backbone network beyond the C-band: Towards multi-band optical networks," IEEE Photon. J., vol.13, no.2, pp.1–18, 2021.

[9] N. Deng, L. Zong, H. Jiang, Y. Duan, and K. Zhang, "Challenges and enabling technologies for multi-band WDM optical networks," IEEE/Optica J. Lightwave Technol., vol.40, no.11, pp.3385–3394, 2022, doi: 10.1109/JLT.2022.3162725.

[10] M. Nakagawa, H. Kawahara, T. Seki, and T. Miyamura, "Adaptive link-by-link band allocation: A novel adaptation scheme in multi-band optical networks," 2021 International Conference on Optical Network Design and Modeling (ONDM), pp.1–6, 2021, doi: 10.23919/ONDM51796.2021.9492502.

[11] D. Saito, Y. Mori, K. Hosokawa, S. Yanagimachi, and H. Hasegawa, "Cost-effective network capacity enhancement with multi-band virtual bypass links," Optical Fiber Communication Conference (OFC) 2023, paper M4G.4, March 2023.

[12] G. Li, N. Bai, N. Zhao, and C. Xia, "Space-division multiplexing: The next frontier in optical communication," OSA Adv. Opt. Photon., vol.6, no.4, pp.413–487, 2014.

[13] P.J. Winzer, "Scaling optical fiber networks: Challenges and solutions," OSA Optics and Photonics News, vol.26, no.3, pp.28–35, 2015.

[14] T. Mizuno and Y. Miyamoto, "High-capacity dense space division multiplexing transmission," Optical Fiber Technology, vol.35, pp.108–117 2017.

[15] J. Sakaguchi, B.J. Puttnam, W. Klaus, Y. Awaji, N. Wada, A. Kanno, T. Kawanishi, K. Imamura, H. Inaba, K. Mukasa, R. Sugizaki, T. Kobayashi, and M. Watanabe, "19-core fiber transmission of 19×100×172-Gb/s SDM-WDM-PDM-QPSK signals at 305 Tb/s," OFC/NFOEC, paper PDP5C.1, March 2012.

[16] T. Kobayashi, M. Nakamura, F. Hamaoka, K. Shibahara, T. Mizuno, A. Sano, H. Kawakami, A. Isoda, M. Nagatani, H. Yamazaki, Y. Miyamoto, Y. Amma, Y. Sasaki, K. Takenaga, K. Aikawa, K. Saitoh, Y. Jung, D.J. Richardson, K. Pulverer, M. Bohn, M. Nooruzzaman, and T. Morioka, "1-Pb/s (32 SDM/46 WDM/768 Gb/s) C-band dense SDM transmission over 205.6-km of single-mode heterogeneous multi-core fiber using 96-Gbaud PDM-16QAM channels," 2017 Optical Fiber Communications Conference and Exhibition (OFC), March 2017.

[17] D. Soma, Y. Wakayama, S. Beppu, S. Sumita, T. Tsuritani, T. Hayashi, T. Nagashima, M. Suzuki, M. Yoshida, K. Kasai, M. Nakazawa, H. Takahashi, K. Igarashi, I. Morita, and M. Suzuki, "10.16-Peta-B/s dense SDM/WDM transmission over 6-mode 19-core fiber across the C+L band," J. Lightwave Technol., vol.36, no.6, pp.1362–1368, March 2018, doi: 10.1109/JLT.2018.2799380.

[18] K. Saitoh and S. Matsuo, "Multicore fiber technology," IEEE/OSA J. Lightwave Technol., vol.34, no.1, pp.55–66, 2016.

[19] K. Saitoh, "Multi-core fiber technology for SDM: Coupling mechanisms and design," J. Lightwave Technol., vol.40, no.5, pp.1527–1543, March 2022, doi: 10.1109/JLT.2022.3145052.

[20] L.E. Nelson, M.D. Feuer, K. Abedin, X. Chou, T.F. Taunay, J.M. Fini, R. Issac, R. Harel, G. Cohen, and D.M. Marom, "Spatial superchannel routing in a two-span ROADM system for space division multiplexing," IEEE/OSA J. Lightwave Technol., vol.32, no.4, pp.783–789, 2013.

[21] M. Jinno, T. Kodama, and T. Ishikawa, "Principle, design, and prototyping of core selective switch using free-space optics for spatial channel network," J. Lightwave Technol., vol.38, no.18, pp.4895–4905, Sept. 2020, doi: 10.1109/JLT.2020.3000304.

[22] H. Takeshita, K. Matsumoto, S. Yanagimachi, and E.L.T. de Gabory, "Configurations of pump injection and reinjection for improved amplification efficiency of turbo cladding pumped MC-EDFA," J. Lightwave Technol., vol.38, no.11, pp.2922–2929, June 2020, doi: 10.1109/JLT.2020.2974483.

[23] D.M. Marom, P.D. Colbourne, A. D'Errico, N.K. Fontaine, Y. Ikuma, R. Proietti, L. Zong, J.M. Rivas-Moscoso, and I. Tomkos, "Survey of photonic switching architectures and technologies in support of spatially and spectrally flexible optical networking," IEEE/OSA J. Opt. Commun. Netw., vol.9, no.1, pp.1–26, Jan. 2017.

[24] X. Cao, C. Qiao, V. Anand, and J. Li, "Wavelength assignment in waveband switching networks with wavelength conversion," GLOBECOM, vol.3, pp.1942–1947, 2004.

[25] J. Yamawaku, A. Takada, W. Imajuku, and T. Morioka, "Evaluation of amount of equipment on single-layer optical path networks managing multigranularity optical paths," IEEE/OSA J. Lightwave Technol., vo.23, no.6, pp.1971–1978, 2005.

[26] I. Yagyu, H. Hasegawa, and K. Sato, "An efficient hierarchical optical path network design algorithm based on a traffic demand expression in a cartesian product space," IEEE J. Sel. Areas Commun., vol.26, no.6, pp.22–31, 2008.

[27] N. Naas and H.T. Mouftah, "On the benefits of traffic bifurcation in multi-granular optical transport networks," 14th Conference on Optical Network Design and Modeling (ONDM), pp.1–6, 2010.

[28] O. Turkcu and S. Subramaniam, "Optical waveband switching in optical ring networks," IEEE INFOCOM, pp.596–604, 2010.

[29] S. Chandrasekhar, C.R. Doerr, and L.L. Buhl, "Flexible waveband optical networking without guard bands using novel 8-skip-0 banding filters," IEEE Photon. Technol. Lett., vol.17, no.3, pp.579–581, March 2005.

[30] S. Kakehashi, H. Hasegawa, K. Sato, and O. Moriwaki, "Formulation of waveguide connection for waveband MUX/DEMUX using concatenated arrayed-waveguide gratings," IEICE Trans. Commun., vol.E90-B, no.10, pp.2950–2952, Oct. 2007.

[31] S. Kakehashi, H. Hasegawa, K. Sato, and O. Moriwaki, "Interleaved waveband MUX/DEMUX developed on single arrayed-waveguide grating," Proc. OFC/NFOEC, Feb. 2008.

[32] Polatis 576x576, https://www.polatis.com/polatis576.asp, accessed July 14th, 2023.

[33] R. Shiraki, Y. Mori, H. Hasegawa, K. Sato, and P. Monti, "Design and control of highly spectrally efficient photonic networks enabled by fiber-granular routing on overlaid ring-shaped topologies," J. Opt. Commun. Netw., vol.13, no.11, pp.233–243, 2021.

[34] H. Hasegawa, S. Subramaniam, and K. Sato, "Node architecture and design of flexible waveband routing optical networks," IEEE/OSA J. Opt. Commun. Netw., vol.8, no.10, pp.734–744, 2016, https://doi.org/10.1364/JOCN.8.000734

[35] T. Ishikawa, Y. Mori, H. Hasegawa, S. Subramaniam, K. Sato, and O. Moriwaki, "Compact OXC architecture, design and prototype development for flexible waveband routing optical networks," Opt. Express, vol.25, no.14, pp.15838–15853, 2017.

[36] J. Wu, M. Xu, S. Subramaniam, and H. Hasegawa, "Joint banding-node placement and resource allocation for multigranular elastic optical networks," IEEE/OSA J. Opt. Commun. Netw., vol.10, no.8, pp.C27–C38, 2018, https://doi.org/10.1364/JOCN.10.000C27

[37] T. Kuno, Y. Mori, S. Subramaniam, M. Jinno, and H. Hasegawa, "Design and evaluation of a reconfigurable optical add-drop multiplexer with flexible waveband routing in SDM networks," IEEE/Optica J. Opt Commun. Netw., vol.14, no.4, pp.248–256, 2022, https://doi.org/10.1364/JOCN.450504

[38] R. Munakata, T. Kuno, Y. Mori, S. Lin, M. Matsuura, S. Subramaniam, and H. Hasegawa, "Architecture and performance evaluation of bundled-path-routing multi-band optical networks," Optical Fiber Communication Conference (OFC) 2023, paper M4G.8, 2023.

[39] M.E. Ganbold, T. Yasuda, Y. Mori, H. Hasegawa, and K. Sato, "Assessment of optical cross-connect architectures for the creation of next generation optical networks," 2018 23rd Opto-Electronics

and Communications Conference (OECC), pp.1–2, July 2018, DOI: 10.1109/OECC.2018.8729881

[40] M. Jinno, K. Yamashita, and Y. Asano, "Architecture and feasibility demonstration of core selective switch (CSS) for spatial channel network (SCN)," OptoElectronics and Communications Conference (OECC) and International Conference on Photonics in Switching and Computing (PSC), Fukuoka, Japan, pp.1–3, July 2019, DOI: 10.23919/PS.2019.8818047

[41] T. Matsuo, R. Shiraki, Y. Mori, and H. Hasegawa, "Design and dynamic control of fiber-granular routing networks with next-generation optical paths," Optical Fiber Communication Conference (OFC) 2022, paper W3F.6, March 2022, https://doi.org/10.1364/OFC.2022.W3F.6

[42] Y. Terada, Y. Mori, H. Hasegawa, and K. Sato, "Highly spectral efficient networks based on grouped optical path routing," Opt. Express, vol.24, no.6, pp.6213–6228, 2016.

[43] K. Kayano, S. Yamaoka, Y. Mori, H. Hasegawa, and K. Sato, "Highly dense elastic optical networks enabled by grouped routing with distance-adaptive modulation," IEEE Photon. Technol. Lett., vol.31, no.4, pp.295–298, 2019.

[44] I. Chlamtac, A. Ganz, and G. Karmi, "Lightpath communications: An approach to high bandwidth optical WAN's," IEEE Trans. Commun., vol.40, no.7, pp.1171–1182, July 1992.

Hiroshi Hasegawa received his B.E., M.E., and D.E. degrees in electrical and electronic engineering from Tokyo Institute of Technology in 1995, 1997, and 2000, respectively. He is currently a professor at the Graduate School of Engineering, Nagoya University, where he was an associate professor from 2005 to 2019. Before joining Nagoya University, he was an assistant professor at Tokyo Institute of Technology from 2000 to 2005. His current research interests include network/node architectures, devices, design and control of photonic networks, multidimensional digital signal processing, and time-frequency analysis. Dr. Hasegawa is a senior member of IEICE and a member of IEEE.